CRYSTAL
GROWTH
& DESIGN

2004
VOL. 4, NO. 4
671−685

Review

Dense Liquid Precursor for the Nucleation of Ordered Solid Phases from Solution

Peter G. Vekilov

Department of Chemical Engineering, University of Houston, Houston, Texas 77204

Received January 5, 2004

ABSTRACT: A line of recent theories and simulations have suggested that the nucleation of protein crystals might, under certain conditions, proceed in two steps: the formation of a droplet of a dense liquid, metastable with respect to the crystalline state, followed by ordering within this droplet to produce a crystal. In this review, I discuss experimental tests of the applicability of this mechanism to the nucleation of ordered solid phases: crystals or linear, planar, branched, or otherwise ordered aggregates of proteins and small molecule materials from solution. The main arguments stem from recent results on the kinetics of homogeneous nucleation of crystals of the protein lysozyme. These results indicate that under a very broad range of conditions the nucleation of lysozyme crystals occurs via a modification of the theoretically postulated mechanism—as a superposition of fluctuations along the order parameters density and structure. Depending on whether the system is above or below its liquid−liquid coexistence line, a density fluctuation may never or may selectively lead to the formation of a dense liquid droplet; in the former case, the high-density region, the "quasi-droplet", is metastable also with respect to the dilute solution. In both cases, the molecules contained in the high-density region may attain an ordered arrangement, i.e., a structure fluctuation is superimposed on the density fluctuation and a crystalline nucleus is obtained. This outlook on the nucleation of ordered solids from dilute phases suggests that the rate of nucleation can be controlled either by shifting the phase region of the dense liquid phase, or by facilitating the structure fluctuations within a dense liquid droplet or quasi-droplet. Results from the literature indicate that the proposed two-step nucleation mechanism and the related tools for nucleation control may be applicable to the formation of crystalline and noncrystalline ordered solid phases of other, protein and nonprotein materials, from solution.

1. Introduction

Formation of ordered solid phases, such as crystals or lower-dimensional ordered arrays in solution underlies geological, industrial, laboratory, and pathophysiological processes.[1−6] It starts with nucleation, in which a tiny embryo of the new phase is formed, Figure 1.[7,8] Nucleation is one of the two major mechanisms of first-order phase transitions—the generation of a new phase from an old phase, which has higher free energy.[9,10] A prominent feature of nucleation is the metastability of the old phase—the transition requires the passage over a free energy barrier.[11] At sufficiently high supersaturations, this barrier vanishes and the old phase becomes unstable, so that an infinitesimal fluctuation of an order parameter, such as density, can lead to the appearance of the new phase. The rate of generation and growth of the new phase is then only limited by the rate of transport of mass or energy. This second process is referred to as spinodal decomposition.[12,13]

The main concepts in the area of equilibrium between large and small phases and the generation of the nuclei of a new phase were introduced by J. W. Gibbs.[7,8] Gibbs considered nuclei of a fluid phase arising from fluctuations of the density in another fluid phase, Figure 2. In further developments, some of the Gibbs's assumptions

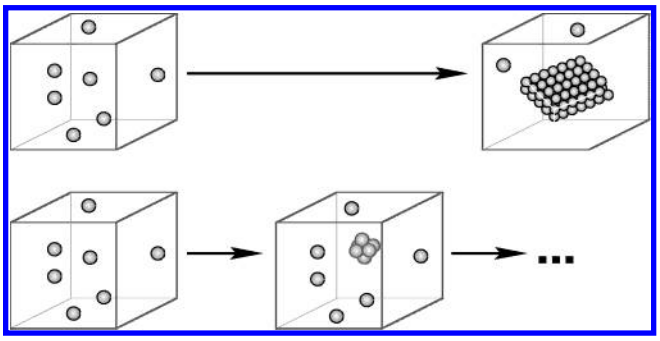

Figure 1. The formation of crystals, whereby a highly ordered phase emerges from a disordered medium, is often viewed as one of the miracles of nature, i.e., one of the most difficult problems to tackle, top. Even the simple picture given by the classical nucleation theory that the crystal starts with a tiny ordered nucleus, bottom, is extremely informative.

10.1021/cg049977w CCC: $27.50
Published on Web 06/04/2004

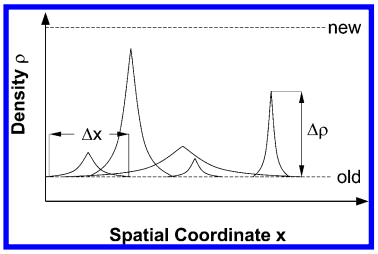

Figure 2. Schematic representation of density fluctuations in a fluid. The free energy of a fluctuation ΔG depends on its characteristic length Δx, and amplitude $\Delta\rho$. Even fluctuations with a density lower than that of the new phase may have $\Delta G \geq \Delta G^*$, the free energy barrier for nucleation, and become nuclei of the new phase. Classical nucleation theory assumes that only fluctuations with $\Delta\rho$ such that $\rho_{old} + \Delta\rho \geq \rho_{new}$ can become nuclei, and defines a critical lengthscale, the radius of the critical nucleus, from the condition $\Delta G \geq \Delta G^*$.

regarding the thermodynamics of nucleation of a fluid phase were transferred to the nucleation of ordered solids, such as crystals, from dilute or condensed fluids, or from other solid states.[14−17] The classical nucleation theory emerged, which assumed, in application to crystals, that the molecular arrangement in a crystal's embryo is identical to that in a large crystal, and hence, the surface free energy of the nuclei will equal the one of the crystal interface. It was also assumed that the size of the nuclei, either the radius, for spherical nuclei, or the side length, for "cubic" clusters, decreases smoothly as supersaturation increases.

There is an inherent contradiction in the application of the Gibbs nucleation theory and its kinetics extensions, see, e.g., refs 16 and 17, to the nucleation of crystals and other ordered solid phases from solution, gas, or other dilute and disordered phases. In Gibbs's considerations, the old and the new fluid phases differ by a single order parameter, density. This is not the case for nucleation of crystals from solution, where at least two order parameters, e.g., density and structure, are necessary to adequately distinguish between the old and new phases.[18] For more than a century, it was implicitly assumed that the transitions along the two order parameters proceed simultaneously, i.e., the building blocks get together in ordered arrays, similar to the schematic in Figure 1. Such an assembly can be described as proceeding along a linear combination of the two characteristic order parameters, and this viewpoint allows the introduction of a unified single-order parameter. This line of thought brings the nucleation of crystals back to the realm of the classical nucleation theory.

Only recently a mechanism of crystal nucleation whereby the density fluctuation precedes the structure fluctuation was suggested by simulations and theory.[19−21] These works concluded that the density and structure fluctuations are separated only near the critical point for liquid−liquid (L−L) separation occurring in the modeled protein solution systems.[19,22,23] For off-critical compositions, the fluctuations along the density and the structure ordered parameters were supposed to occur simultaneously,[19] similarly to the classical viewpoint.

Here I review recent results on crystal nucleation in a protein crystallization system in which a metastable equilibrium between a low- and high-density solutions, L−L separation, occurs in solutions supersaturated with respect to the crystals. The nucleation kinetics data cover the phase space above and below the L−L coexistence line, far and near the critical point for L−L separation. On the basis of the reviewed results, I conclude that a crystal nucleus appears when a structure fluctuation occurs within a region of higher density of molecules existing for a limited time due to a density fluctuation, i.e., a structure fluctuation is superimposed on a density fluctuation. The conclusion about the action of this mechanism under conditions in which L−L separation is not observed (the dense liquid phase is either unstable, or has a short lifetime in a metastable state) has broad implications for protein and nonprotein systems, which do not exhibit L−L phase separation. It correlates with results showing the applicability of this mechanism not only to proteins, but also to small molecule systems.[24,25] While some of the tested materials have phase diagrams similar to those of proteins, with a L−L separation submerged below the solution−crystal equilibrium,[25] in other cases no observable dense liquids exist.[24] As an interesting aside, it was found that near the critical point for L−L separation, the solution gels and all kinetics, including nucleation, are arrested, a scenario not envisioned in the original theoretical works.[26]

2. Determination of the Nucleation Rate

For insight into the nucleation mechanism at moderate and high supersaturations, and on the effects that potential dense liquid phase may have on the nucleation of crystals, I use data on the kinetics of homogeneous nucleation of crystals of the protein lysozyme.

Some of the methods for determinations of homogeneous nucleation rates applied to inorganic crystals would be inapplicable or produce ambiguous results if applied to protein systems. For instance, different variants of cloud chamber[27] and supersonic nozzle expansion techniques[28] are specific for vapor−liquid nucleation. Techniques that use levitating droplets[29,30] are prone to evaporation of solution from the liquid−air interface and may lead to biases due to effects of the electromagnetic or acoustic fields on the nucleation process.[31]

Direct counting of protein crystals grown to optically detectable size in supersaturated solutions[32−36] allows rough evaluations of the nucleation rate, J (in units $cm^{-3}\ s^{-1}$), i.e., the number of stable nuclei appearing in a unit volume per unit time. These studies, however, are limited to the overall number of crystals, thus giving only an integral of J over time and supersaturations and do not account for the inevitable heterogeneous nucleation events.[37]

Another method applied to identify nucleation events has been dynamic light scattering.[38,39] The method was used with several proteins and protein complexes: ferritin, pumpkin seed globulin, and the satellite tobacco mosaic virus, whose size is sufficiently large so that even small clusters can be detected by dynamic light scattering. In a supersaturated solution, with time a signal indicating the appearance of aggregates larger than the size of one molecule appears. The average size of the aggregate was found to slowly increase. These aggregates have been assumed to correspond to precritical

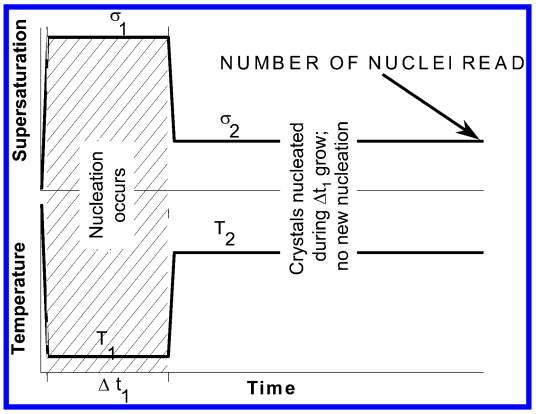

Figure 3. Temperature regimes and corresponding supersaturation levels used to induce nucleation during the time Δt_1 and to develop the crystals to detectable dimensions for a system with normal temperature dependence of the solubility, such as lysozyme used here.

clusters, and in this way the time evolution of the precritical sizes has been monitored for several proteins.[38,39]

In pursuit of data allowing definitive conclusions about the nucleation mechanism, a novel technique that allows direct determinations of the steady-state rate of homogeneous nucleation was recently developed. In the beginning of an experiment run, the temperature is lowered to a selected T_1 at which nucleation occurs, Figure 3. After a time period of Δt_1 temperature is raised from the nucleation temperature T_1 to the growth temperature T_2. The temperature T_2 is chosen so that the supersaturation is at a level in which nucleation rate is practically zero, but the crystals already formed can grow to detectable dimensions.[40] This regime allows nucleation to occur at constant supersaturation during Δt_1 at T_1 without solution depletion due the growth of the nucleated crystals—growth predominantly occurs during the significantly longer times at T_2. After the growth stage, the crystals nucleated at T_1 during Δt_1 are counted.

To obtain reproducible statistical characteristics of the random nucleation process, 400 simultaneous trials take place under identical conditions, in solution droplets of volume 0.7 μL. To suppress the undesired nucleation at the solution/air interface, the droplets were suspended in inert silicone oil, used in optimizations of the crystallization conditions of a variety of proteins.[41] To extract the nucleation rate from the time dependence of the number of nucleated crystals, five arrays of 400 droplets are subjected to the nucleation supersaturation at increasing time intervals Δt_1. These Δt_1's ranged from 12 min to, at the lowest supersaturations, 8 h. Thus, the determination of one nucleation rate data point is based upon statistics of over 2000 protein solution droplets. The experiment setup, experimental and data collection procedures, and the extensive tests to validate this technique are discussed in detail in refs 37 and 42.

Although the number of crystals in a droplet is a random variable, Figures 4 and 5, the mean number of nucleated crystals is reproducible and increases linearly with time, see Figure 6 and ref 43, indicating steady-state nucleation at the chosen experimental conditions. Although heterogeneous nucleation was significantly reduced through various precautions,[37,42,43] apparently

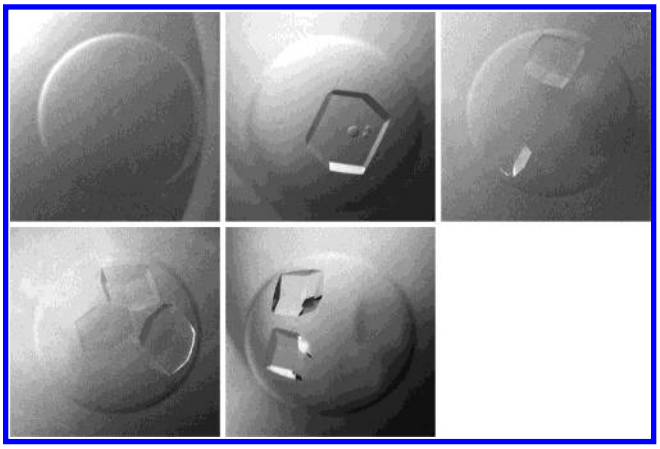

Figure 4. Variations in the number of crystals nucleated in a droplet between none and four under identical conditions. Width of images 1.25 mm. Reprinted with permission from ref 42. Copyright 1999.

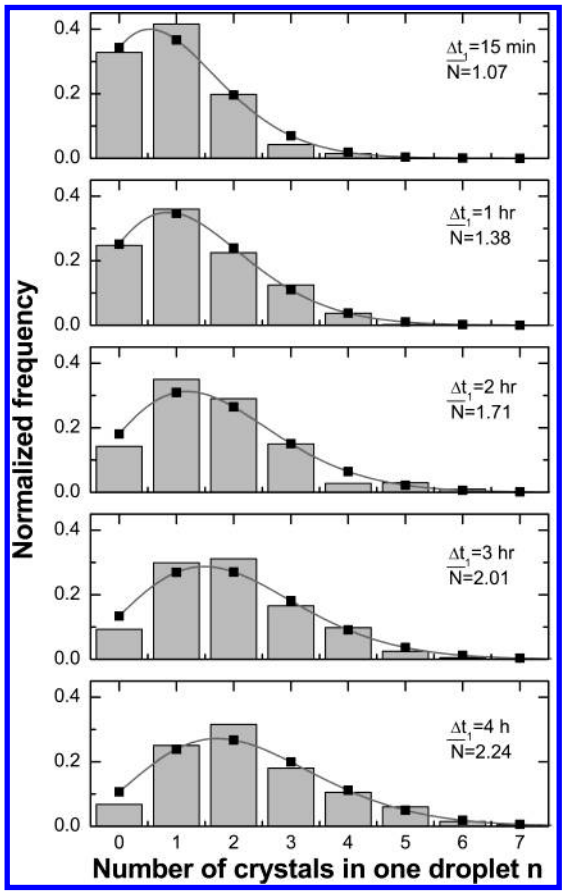

Figure 5. Distributions of the number of lysozyme crystals n appearing in one droplet as a result of increasing nucleation times Δt_1 indicated in the plots. Each distribution presents the result of simultaneous experiments in 400 droplets with volume $V = 0.7$ μL each, lysozyme concentration $C = 55.5$ mg mL^{-1}, precipitant NaCl concentration $C_{NaCl} = 3\%$. Bars: experiment results; lines and symbols: fits with Poisson distribution. Reprinted with permission from ref 43. Copyright 2000.

it still occurs—note the nonzero intercept of the data in Figure 6 at $t = 0$. Likely centers for this process may be the small (<0.22 μm) particles remaining in the solution after filtration. The good linearity of the $N(t)$ at $t > 0$ indicates that the heterogeneous nucleation is limited to times shorter than those accessible to our

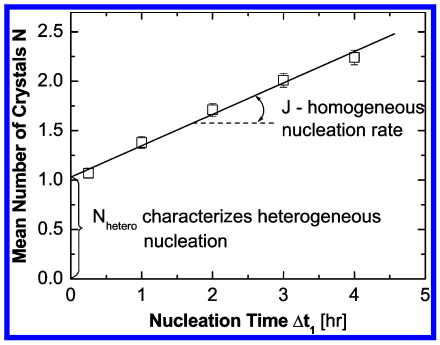

Figure 6. Time Δt_1 dependence of the mean number of crystals in one droplet N. Each N value is determined from the Poisson distributions for simultaneous experiments in 400 droplets with volume $V = 0.7\ \mu$L, lysozyme concentration $C =$ 55.5 mg mL^{-1}, precipitant NaCl concentration $C_{NaCl} = 2.5\%$. Error bars correspond to $\sqrt{N/N_{trial}}$. The slope of the straight line is used to calculate the nucleation rate J in cm^{-3} s^{-1}, and the intercept N_{hetero} characterizes heterogeneous nucleation. From ref 42.

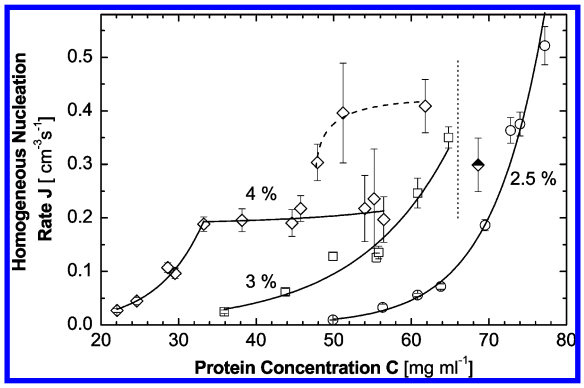

Figure 7. Dependencies homogeneous nucleation rates J of lysozyme crystals on protein concentration C at $T = 12.6$ °C and the three precipitant concentrations C_{NaCl} indicated in the plots. Solid lines − fits with exponential functions; dashed line for data points at $C_{NaCl} = 4\%$ is just a guide for the eye. Datum point at $C_{NaCl} = 4\%$ and lysozyme $C = 68$ mg mL^{-1} was obtained in a cloudy solution and was not used in fitting procedures. Vertical dotted line at $C = 66$ mg mL^{-1} indicates the L−L demixing boundary at this T and $C_{NaCl} = 4\%$. Reprinted with permission from ref 43. Copyright 2000.

technique. This mode of fast crystal nucleation leads to a constant additive to the number of nucleated crystals at all times. Thus, the intercept of the dependence with ordinate axis in Figure 6 can be used to characterize the rate of *heterogeneous* nucleation and the slope of this dependence yields the *homogeneous* nucleation rate.

3. Kinetics of the Nucleation Processes

The variations of the homogeneous nucleation rate of lysozyme crystals with protein concentration at three different concentrations of the precipitant, NaCl, determined with the direct method discussed above, are presented in Figure 7. In agreement with general expectations, the nucleation rate increases exponentially with protein concentration at each precipitant concentration, and, overall, is higher at higher precipitant concentrations. However, at the highest precipitant concentration, $C_{NaCl} = 4\%$, the $J(C)$ dependence contains three peculiarities.

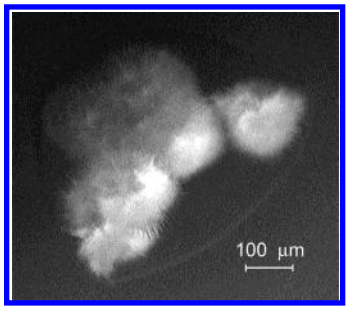

Figure 8. "Sea urchin" morphology of crystals observed in a few of the droplets during runs at $C_{NaCl} = 4\%$ and $T = 12.6$ °C yielding higher J's, as well as the run at $C_{NaCl} = 4\%$ and lysozyme $C = 68$ mg mL^{-1} in which the crystals nucleated in a cloudy solution. Reprinted with permission from ref 43. Copyright 2000.

(i) The dependence breaks at $C^* = 33.5$ mg/mL, with the sections at $C < C^*$ and $C > C^*$ following different exponents.

(ii) At $C > 48$ mg/mL, the dependence bifurcates with the data points belonging to either of two branches. In the runs leading to J's from the upper branch, in a few droplets (∼2−3 out of ∼2000) spherulitic crystals, similar to those in Figure 8, were noticed. This suggests that the closeness of the L−L coexistence boundary may be affecting crystallization in those runs.[44]

(iii) The data point at the highest lysozyme concentration, $C = 68$ mg/mL and $C_{NaCl} = 4\%$ is lower than the data point determined at lower C and C_{NaCl}, 64 mg/mL and 3%, respectively. During the determination of the data point at $C_{NaCl} = 4\%$, the crystallization solutions in all 2000 droplets became cloudy immediately after temperature was lowered to the nucleation temperature and became clear again when T was raised to T_2. This indicates that this set of conditions (C, C_{NaCl}, T) is below the L−L coexistence boundary for the lysozyme−water−NaCl system, see phase diagram in Figure 9. After the growth stage, most of the crystals found in the droplets appeared like regular tetragonal lysozyme crystals. However, in a few (∼20 out of 2000) droplets spherulitic crystals with thin needles growing radially outward from a center ("sea urchin" morphology) were detected, see Figure 8. No correlation between the nucleation times and the number of droplets with "sea urchin" morphology crystals was found. The presence of crystals with such unusual shape has been related to crystallization starting below the L−L coexistence line.[45]

4. The Nucleus Size

To understand the breaking of the nucleation rate dependencies on the supersaturation, we link them to the response of the nucleus size to supersaturation. The nucleus or critical cluster of the new phase is a cluster that has equal probability to grow or to dissolve and is in a labile equilibrium with the supersaturated solution.[46−49] The number of molecules in the nucleus is an important characteristic of the nucleation process. The nucleus size and shape largely determine the height of the free energy barrier for nucleation (i.e., the reversible work for nucleation), ΔG^*, and hence the nucleation rate J. The relation between ΔG^* and the excess number of molecules in a solution volume holding the nucleus n^* over those in an equal solution volume

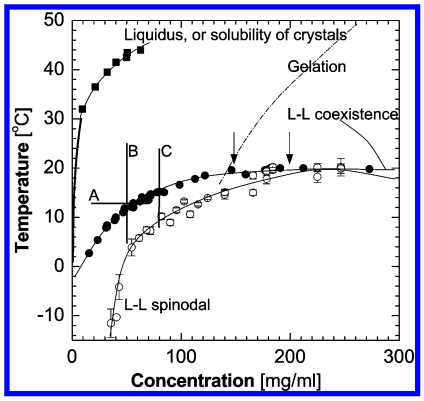

Figure 9. A section of the phase diagram of lysozyme solutions in the presence of 4% NaCl. As shown in refs 23, 77, and 102 for many proteins the L−L coexistence line is below the liquidus line because of the very short range of attractive interactions. The L−L coexistence line and the corresponding spinodal are from ref 116. Error bars for L−L binodal are within the size of the symbols. Solubility of tetragonal crystals at low lysozyme concentrations calculated using empirical formula from ref 71. Solubility at higher lysozyme concentrations—independently measured using methods discussed in ref 117. Error bars are smaller than symbol size. Lines A, B and C mark conditions used in the studies reviewed here. Arrows mark concentrations at which the determinations of the nucleation rate were hampered by the onset of gelation. Approximate location of gelation line marked with dash−dotted line.[45]

without the nucleus n_0, is treated by the nucleation theorem of Kashchiev and Oxtoby,[50,51] a universal, model-independent nucleation law. Since the nucleation work ΔG^* can be estimated from the logarithm of the nucleation rate J, in terms of J and n^* the nucleation theorem becomes

$$n^* - n_0 = k_B T \frac{\partial \ln J}{\partial \Delta\mu} + \alpha \qquad (1)$$

where α is a correction that takes values between 0 and 1.[51]

To present the dependencies of the nucleation rates on the concentrations of the protein and precipitant in Figure 7 in the variables of the nucleation theorem, the data were replotted in Figure 10 in terms of functions of thermodynamic supersaturation σ.

Figure 10b indicates that at $C_{NaCl} = 2.5$ and 3% n^* does not change throughout the respective supersaturation ranges, while at $C_{NaCl} = 4\%$ the nucleus size changes abruptly at $\sigma = 3.1$, corresponding to $C = 33.5$ mg/mL. The values of $n^* - n_0$ extracted from the four linear segments in Figure 10b are shown in Table 1. Since supersaturation is defined as the logarithm of the ratio of C to C_{eq}, the exact value of C_{eq} does not affect the slope of the straight lines in Figure 10b. Hence, the values of $n^* - n_0$ are independent of possible experimental errors of the solubility measurements.

To roughly evaluate n_0, the molecular diameter, ~30 Å, was compared to the distance between the molecular centers $n_1^{-1/3}$, where n_1 is the protein *molecular* concentration. At $C \approx 70$ mg/mL, $n_1 = 2.9 \times 10^{18}$ cm^{-3} and the distance is ≈70 Å. At 2.5% NaCl and a protein concentrations close to 70 mg/mL, in the volume occupied by a crystal consisting of ~10 molecules, there may be at most $n_0 \approx 1$ solute molecule. At the other

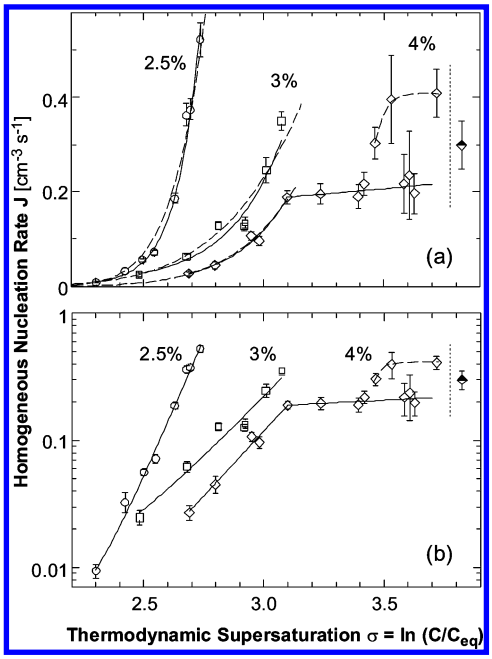

Figure 10. Dependencies of homogeneous nucleation rate J on supersaturation $\sigma \equiv \Delta\mu/k_B T$ at $T = 12.6$ °C and at the three precipitant concentrations indicated on the plots. Solid lines − fits with exponential functions; dashed lines fits with the classical nucleation theory expression, eq 1. Data points with higher J's at $C_{NaCl} = 4\%$, and datum point obtained in a cloudy solution at $C_{NaCl} = 4\%$ and lysozyme $C = 68$ mg mL^{-1} were not used in fitting procedures; see text for details. Vertical dotted lines at $\sigma = 3.9$ indicate the L−L demixing boundary at this T and $C_{NaCl} = 4\%$. (a) Linear coordinates; (b) semilogarithmic coordinates. Reprinted with permission from ref 43. Copyright 2000.

Table 1. Characteristics of Nucleation Process Determined from Fits of Eqs 2−5 to Data[a]

C_{NaCl} (%)	$n^* - n_0$	A [s^{-1}]	B	γ [mJ/m^2]	n^*_{CNT}
2.5	9.6 ± 0.2	(9 ± 5) × 10^{-16}	65 ± 4	0.64	11−7
3	4.2 ± 0.2	(4 ± 2) × 10^{-18}	33 ± 4	0.51	4−2
4	4.7 ± 0.3	(1.4 ± 0.7) × 10^{-17}	44 ± 4	0.56	5−3
4	0.2 ± 0.3				

[a] For definitions and details, see text.

precipitant concentrations, the $n^* - n_0$ values in Table 1 and the volume occupied by the nuclei are smaller; hence, n_0 is smaller and the correction it introduces in the nucleus size is comparable or smaller than α. With this in mind, the n^*'s corresponding to the $n^* - n_0$ values in Table 1 were extracted: for $C_{NaCl} = 2.5\%$ n^* is 10 or 11, at $C_{NaCl} = 3\%$, $n^* = 4$ or 5, at $C_{NaCl} = 4\%$, $n^* = 4$ or 5 and then 1 or 2 molecules.

Critical clusters consisting of one molecule have been encountered before in investigations of electrochemically driven nucleation of new phases under high overvoltages/supersaturations.[52,53] Similar to the case of nucleation of lysozyme crystals, it was concluded that the nucleation rate is determined only by the kinetics of attachment of molecules to this critical cluster. The lack of a thermodynamic barrier for the formation of nuclei of the new phase in this regime makes it similar to spinodal decomposition. This similarity can lead to deeper insights into the mechanism of the phase transition and the pathways to control the spatiotemporal

structure of the new phase; it merits detailed further investigations.

5. Comparison with Predictions of Classical Nucleation Theory

The classical nucleation theory (CNT) assumes that (i) the cluster size changes continuously around the critical region, (ii) the structure of the near-critical clusters is identical to that of large crystals, and (iii) their shape is determined by minimization of their surface free energy. These are good approximations to reality only for large nuclei. The observed transition from critical cluster sizes of 10 to 4 to 1 contradict assumption (i). Obviously, clusters so small cannot have the structure of a large tetragonal lysozyme crystal, and this is a contradiction to assumption (ii). Last, with such small clusters, rearrangements of the molecules within a cluster will lead to major variations of its total free energy that take it out of the critical region. They cannot by viewed as fluctuations of the shape of the critical cluster that will result in a shape minimizing its free surface energy, a contradiction to assumption (iii).

Thus, the size of the nuclei determined above precludes application of classical theory to our data. We compare below the experimental results to the predictions of this theory only to illustrate that good correspondence between experimentally determined $J(T)$ dependencies and the predictions of the classical theory should not be used as a proof that nucleation follows the mechanism assumed by the classical nucleation theory.

Within the framework of the classical nucleation theory, the dependence of the nucleation rate on supersaturation σ and protein molecular concentration n_1 is[33,54]

$$J = An_1 \exp(-B/\sigma^2) \tag{2}$$

The coefficient A is a complicated function of the molecular-level attachment-kinetics parameters. There have been attempts to analytically derive an expression for this coefficient for nucleation from solution.[15−17,55] In all cases, the final formulas for A contain variables that are often impossible to determine independently.

The parameter B is related to the thermodynamic barrier for the creation of the critical cluster ΔG^* and for a spherical cluster can be written as

$$B = \frac{16\pi}{3}\frac{\Omega^2\gamma^3}{(k_B T)^3}, \tag{3}$$

where Ω is the protein molecular volume in the crystal and γ is the surface free energy of the critical cluster. Two-parameter fits of our data with eq 2. in Figure 10a show reasonably good correspondence. The best-fit values of A and B are shown in Table 1. From the values of B, we estimate the surface free energy γ, also shown in Table 1.

Classical nucleation theory also allows determinations of the nucleus size as

$$n^*_{CNT} = \frac{2B}{\sigma^3} \tag{4}$$

This size continuously changes in the supersaturation ranges of the experiments. The nucleus sizes determined using eq 4 straddle the more accurate determinations based on the nucleation theorem, eq 1. This correspondence seems to support the general belief that CNT provides a fair estimate for the nucleation barrier and the nucleus size, even under conditions in which its inapplicability is unquestionable.[56−58]

With this limited adequacy in mind, we can address the estimates of the surface free energy γ of the nuclei, in the range 0.5−0.7 mJ m^{-2}. These values are about 2 orders of magnitude lower than the respective values for inorganic crystals. However, if rescaled with the area that a protein molecule occupies on the surface of a crystalline nucleus, one gets values of the energy of the "dangling" bonds per molecule similar to those for inorganic crystals,[39] and this agrees with expectations for the combination of hydrogen, van der Waals, ionic, and other bonds that underlie both protein and water-soluble small-molecule crystals.

6. Liquid−Liquid Separation and Crystal Nucleation

The peculiarities of the nucleation kinetics discussed above suggest that the nucleation at high supersaturations is affected by the L−L separation of the protein solution. To understand L−L separation we start with the fact that the ranges of the various types of interactions possible between protein molecules in solution are shorter than the protein molecular sizes.[23] This ratio of the two characteristic lengthscales has been evidenced in numerous studies,[59,60] and can be viewed as a consequence of the fact that all interactions, other than the electrostatic, necessarily scale with the size of the water molecules, ∼2 Å. The electrostatic interactions at any ionic strength higher that 0.1 M have a decay length of <10 Å,[44] i.e., again shorter than the sizes of even the smallest proteins molecules of ∼30 Å.

To a large extent, the short interactions' range determines the typical phase diagram of protein solutions.[23,61] For spherical colloids, it has been shown that the range of attraction has a drastic effect on the phase diagram.[62] If the range of attraction is longer than the particle diameter, the phase diagram of the colloidal suspension resembles that of a typical atomic substance,[19] with three stable phases co-exiting in pairs and triple point. These are a dilute fluid analogous to the vapor phase, a dense fluid analogous to the liquid phase, and a crystal phase, depending on the temperature and density of the suspension.[63] However, when the range of the attraction is reduced, the fluid−fluid line moves toward the line where the solid coexists with the dilute and dense fluid phases. If the range of attraction is made even shorter (less than 25% of the colloid diameter), two stable phases remain, one fluid and one solid.[19] The fluid−fluid coexistence curve survives in the metastable regime below the fluid−solid coexistence curve.[63,64]

These phenomena, while introduced for colloid systems, directly relate to solutions of proteins and nonprotein materials. Several experimental studies with proteins have found phase diagrams very similar to the one expected for colloids with short-range attraction.[22,45,65−67] Such phase diagrams, with L−L

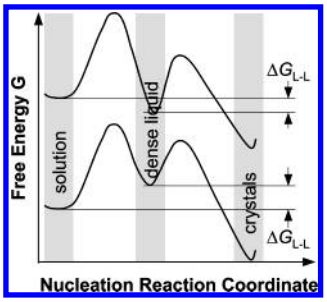

Figure 11. The free-energy G along two possible pathways from solution to crystal. Intermediate minimum is for the quasi-droplet of dense liquid formed as a result of a density fluctuation, final minimum for crystals corresponds to structuring of dense liquid. ΔG_{L-L} is the free-energy of formation of the dense liquid phase: for upper curve, $\Delta G_{L-L} < 0$ and the dense phase is stable respect to initial solution, but metastable with respect to the crystals, i.e., the system is below the L−L coexistence line; for lower curve, the system is above the L−L coexistence line, $\Delta G_{L-L} > 0$, the dense phase is metastable with respect to both the solution and the crystals and only exists as a density fluctuation of a limited lifetime.

phase separation occurring at lower temperatures and metastable with respect to the liquid−solid equilibrium, were also found for fullerenes[68] and some organic molecules.[25]

Along with the three phases expected from the analogy to colloid systems, the studies of the protein phase diagrams found a few novel phenomena. At higher protein concentrations, even above the critical temperature for L−L separation, protein solutions often gel.[45] Recent theory and simulation attribute this gelation to the action of additional, long-range attractive forces.[26,69]

Furthermore, like all other L−L separations,[70] the formation of dense protein liquid phases should have two-phase lines: the coexistence curve, or binodal, and a spinodal, below which the metastable dense liquid forms instantaneously.[22] The phase diagram of the system discussed here: lysozyme−4% NaCl−water at pH = 4.5 maintained by acetate buffer, is shown in Figure 9. It contains low- and high-density liquid phases, the spinodal for the formation of the dense liquid phase, the solubility[71] (or liquidus) line, and the gelation boundary. The L−L binodal is experimentally detected by direct microscopic observation of the clouding and declouding in a protein solution.[45,66,72] The temperature of the spinodal is determined for a given solution compositions by static light scattering[22,73] by extrapolating the temperature dependence of the reciprocal intensity I^{-1} of the scattered light to the temperature where I^{-1} reaches zero.[72] For 3% NaCl, all three phase lines are shifted to lower temperature by ~8 °C.[44]

The thermodynamic and kinetic factors of the L−L and liquid−solid-phase separation have distinct characteristics in different regions of the phase diagram in Figure 9. In the area below the L−L coexistence line, the dense liquid phase is metastable with respect to the crystals and $\Delta G_{L-L} < 0$; however, it has lower free energy and is stable with respect to the low-density solution, Figure 11. The low- and the high-density states are separated by a free energy barrier, whose height determines the rate for formation of the dense liquid. The kinetics of crystallization, limited by another free energy barrier, is slower by many orders of magnitude than the kinetics of formation and decay of dense liquid droplets—dense liquid droplets appear within a few seconds, while crystal nucleation takes days. Thus, on its way to lower the free energy of the supersaturated low-density solution, the system stops at the state of the dense phase. A metastable equilibrium between the low- and high-density liquids is obtained. This allows the dense phase droplets to grow to detectable dimensions. As discussed above, the only difference in this scenario below the L−L spinodal is that the barrier separating the low- and high-density solution vanishes, and the formation of the dense liquid droplets is instantaneous.

Above the L−L coexistence line, the free energy of the dense liquid is, obviously, higher than the free energy of the low-density solution. However, a local minimum, corresponding to a dense liquid metastable with respect to both crystals and low-density solution is likely, especially in the area immediately above the L−L separation line, Figure 11, with $\Delta G_{L-L} > 0$. Some of the inevitable density fluctuations reach this minimum. Because of the driving force for decay into the low-density solution and the fast kinetics of this decay, the doubly metastable dense liquid existing in this minimum has a limited lifetime. This does not allow the density fluctuations to grow to detectable droplets. The results reviewed below show that this doubly metastable dense liquid is a crucial first step in the mechanism of nucleation of crystals from solutions in the area above the L−L separation line or in systems, in which long-lifetime dense liquid, metastable only with respect to the crystals, does not exist.

7. Nucleation Rates and the Solution Phase Diagram

The line A in Figure 9 shows the locations in the (T,C) plane of all nucleation experiments discussed above. The experimental conditions are far from the L−L separation curve for $C_{NaCl} = 3\%$ and should be even further away for $C_{NaCl} = 2.5\%$. Thus, one should not expect any effects of the L−L demixing on the nucleation of crystals at these two precipitant concentrations. Correspondingly, no solution clouding or spherulitic crystals were found in these series of experiments. However, the line A crosses the L−L separation curve for $C_{NaCl} = 4\%$. The data point at this precipitant concentration and $C = 68$ mg/mL in Figure 7 was recorded below this curve in the region of L−L coexistence, and, correspondingly, during nucleation, the solution was cloudy. The slower crystal nucleation in the region of L−L coexistence correlates with the observations discussed below and is an important point for the understanding of the role that dense liquid phases play in crystal nucleation.

As shown below, the vicinity of the L−L separation boundary is a location of enhanced nucleation of crystals. Minor variations of the solution composition that cause small changes in the locations of the L−L curve may have a strong effect on the nucleation rate. We attribute the kinetic instability in $J(C)$ for $C > 48$ mg/mL to such variations.[43]

8. Enhanced Nucleation above T_{L-L}

To further probe the effects of the dense liquid phase on the nucleation of the lysozyme crystals, we carried

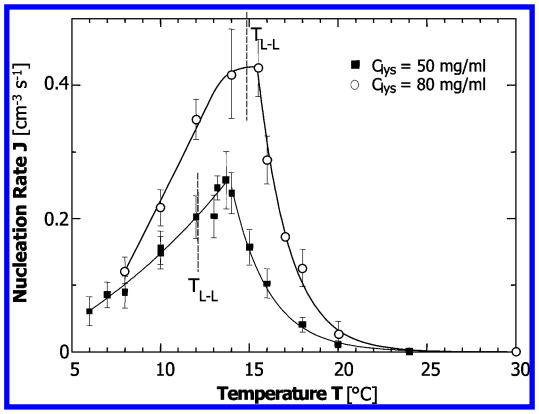

Figure 12. Dependencies of the rate of homogeneous nucleation of lysozyme crystals J on temperature T at pH = 4.5 by 50 mM sodium acetate buffer and 4% (w/v) NaCl. ■ − lysozyme concentration C_{lys} = 50 mg mL^{-1}, ○ − C_{lys} = 80 mg mL^{-1}. Vertical dotted lines indicate respective temperatures of L−L separation T_{L-L}. Curves are just guides for the eyes. Reprinted with permission from ref 43. Copyright 2000.

out a series of experiments, in which we kept the concentration of the protein constant and crossed into the L−L coexistence region by lowering the temperature. In these experiments, we use L−L separation as a probe for the mechanisms of crystal nucleation that operate not only in the vicinity of the L−L separation phase region, but also away from it.

Figure 12 presents the dependencies of the homogeneous nucleation rate J on the temperature T recorded at two protein concentrations. The conditions of these experiments are represented with lines B and C in the phase diagram in Figure 9. In all cases, we see that as T is lowered, J increases, reaches a maximum near the respective T_{L-L}, and then decreases even above the L−L separation region.

Experiments at protein concentrations of 150 and 200 mg/mL revealed the expected[19,20] extremely high crystal nucleation rates close to (C^{crit},T^{crit}). However, a few minutes after T was lowered to the chosen value, solution gelation[45,64] occurred and, accordingly,[74] nucleation was arrested. These observations indicate that, strictly speaking, the enhancement of the crystal nucleation at the critical point for L−L separation predicted by the theory and simulations in refs 19−21 does not occur.

While the exponential increase in $J(T)$ before the maximum is readily linked to higher frequency and amplitude of both density and structure fluctuations as the temperature is lowered away from $C_e(T)$, the maxima and the subsequent decreasing branches show that

(i) Since the maxima in $J(T)$ curves follow the location of the L−L separation phase line, we conclude that the dense liquid is a part of the crystal nucleation mechanism.

(ii) Since in both cases the maxima occur at temperatures higher by 1−1.5 °C from the respective T_{L-L}'s, we conclude that dense liquid droplets with long lifetimes existing below the L−L separation line in Figure 9 are not a prerequisite for the nucleation of crystals, and the role of the dense liquid phase for the nucleation mechanism is far from the simplified scenarios, discussed below.

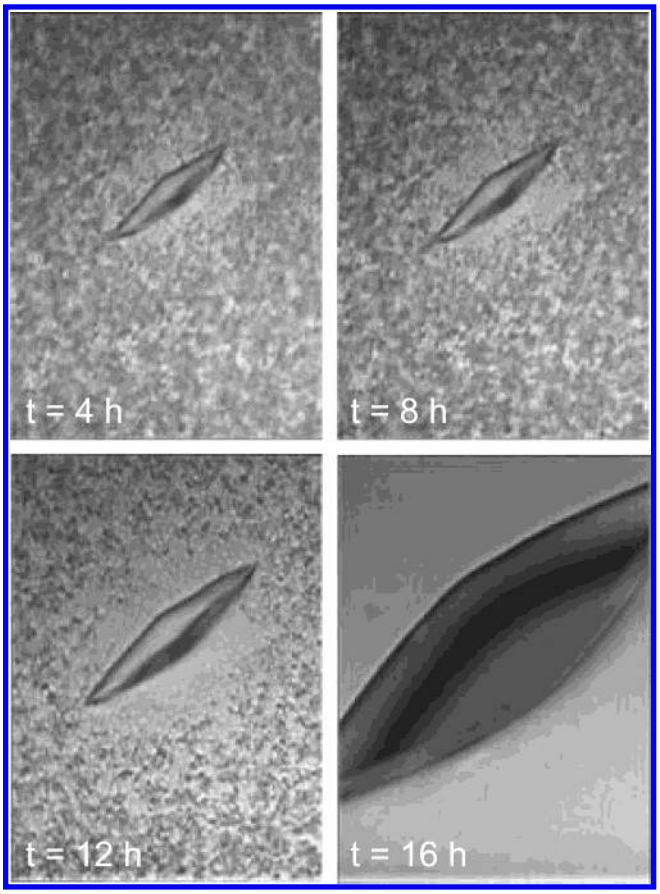

Figure 13. A single tetragonal crystal of lysozyme grows while surrounded by numerous droplets of the dense liquid phase at C_{lys} = 80 mg mL^{-1} and T = 12 °C. Time on frames is measured from the moment in which T was set at its value. Crystal fills ∼20 μm space between two coverslips and its shape is accordingly distorted.

9. Mechanisms of Nucleation Enhancement around $T_{L-L}(C)$

The simplest mechanism that has been invoked to explain the enhancement of nucleation by the dense liquid phase is the higher protein concentration in it. Although appealing in its obviousness, this mechanism fails to explain the decrease in nucleation rate seen in Figure 12 at temperatures deeper into the L−L coexistence region. Further evidence that the presence of long-lifetime droplets of dense liquid is not a prerequisite for enhanced nucleation comes from Figure 13. It shows that the numerous dense liquid droplets do not cause the nucleation of new crystals. A single crystal, present from the beginning of the monitoring period grows and the recruitment of material into it leads to gradual disappearance of the dense liquid droplets. The coupled growth and dissolution are possible because the solubility of the crystals, see Figure 9, is significantly lower than the concentration of the solution in equilibrium with the dense phase; this observation is an illustration of the metastability of the dense liquid phase with respect to the crystals, illustrated in Figure 11. The transfer of protein molecules from the dense liquid phase to the crystals shows that the protein in the droplets is not denatured, and the reason for suppression of nucleation should be sought elsewhere.

It has been suggested that L−L phase separation in a solution supersaturated with respect to crystals may

affect the crystal nucleation in two ways:[19,75] (i) The high-amplitude density fluctuations around the critical point for L−L phase separation (critical density fluctuations) serve as a first stage in the crystal nucleation process, upon which a structure fluctuation is readily superimposed. (ii) The dense liquid-phase wets the crystalline nucleus, and in this way lowers its free surface energy and the related nucleation barrier. Our experiments, carried out at off-critical compositions, allow distinction between these two scenarios. Thus, "wetting" should start at the L−L binodal, and increase upon lowering of temperature in the region of L−L coexistence, while density fluctuations reach their maximum for the chosen solution composition at the L−L spinodal. For this, we correlate the $J(T)$ dependencies in Figure 12 to the phase diagram in Figure 9.

To evaluate the role of the density fluctuation, we note that Figure 9 shows that the L−L spinodal is below the L−L coexistence line by 2−8 °C, depending on the protein concentration. At the concentration of 50 mg mL^{-1} of the experiments in Figure 12, the maximum in $J(T)$ occurs at temperature higher by ∼6 °C from the temperature of the spinodal. At $C = 80$ mg mL^{-1}, the descending branch of $J(T)$ below the L−L coexistence line crosses the spinodal at $T = 9.5$ °C. There is no enhancement of nucleation at that temperature. Thus, we conclude that high-amplitude density fluctuations alone do not contribute to higher nucleation rates.

It is tempting to use the illustrative concept of wetting to describe the enhancement of the nucleation of crystals in the area around the L−L separation boundary.[19,75,76] However, it does not correspond to the data on lysozyme nucleation discussed here—if the liquid wets the crystal nucleus, lowers its surface energy, and thus decreases the nucleation barrier, it is hard to understand why this does not occur at temperatures below T_{L-L}. Furthermore, as pointed out above, the critical cluster consists of as few as 10, or 4 or 1−2 molecules—with so few molecules, it would be difficult to assign some of them to the crystal, and others to the liquid that wets it. Note that the calculation of the nucleation rates in ref 19 was based on a model phase diagram that has been shown to underestimate the separations between the liquidus and the L−L coexistence lines.[23,77,78] As a result, the size of the crystal nucleus near the L−L coexistence line, emerging from the simulations, was unrealistically large, and one could speculate that it could accommodate a liquid layer wetting a crystalline nucleus. The overall conclusion from these considerations is that the macroscopic concepts of wetting or surface tension are not readily applicable to the nucleation of protein solid phases.

There is abundant evidence in the literature that shows that the long-lifetime macroscopic dense liquid phase *does not* promote the nucleation of crystals.[79] In many cases, similar to the example discussed above, crystals and dense liquid droplets were found to coexist for extended periods of time without the droplets generating additional crystal nuclei. In some cases, crystals that were nucleated on the droplet boundaries grew into the dilute solution, rather than into the dense liquid.[79]

For understanding of the suppression of crystal nucleation in dense liquid phases, we note that for some systems, the presence of dense liquid does facilitate the nucleation of ordered solid phases. Figure 14 shows an example of nucleation of bundles of linear arrays, often called polymers, of deoxy-hemoglobin S; the formation these polymers is the primary pathogenic event in the deadly sickle cell anemia.[5,80−83] The temperature is changed from a value at which the dense liquid is the main phase coexisting with the normal solution, to a value where the dense liquid droplets are unstable and the polymers are in equilibrium with the solution; for further details, see ref 84. Smaller droplets disappear within several seconds, while the larger droplets, that have not disappeared, serve as centers for nucleation of deoxy-HbS polymers. Additional spherulites emerge at the locations where the smaller droplets have been, likely due to high deoxy-HbS concentrations undissipated within the short times for the onset of polymerization. This last observation allows us to attribute the enhanced nucleation of polymers in the dense liquid droplets to the higher hemoglobin concentration in them.

The comparison with hemoglobin S allows us to attribute the suppression of nucleation of lysozyme crystals within the dense liquid to the high viscosity of the lysozyme dense liquid.[74] This high viscosity is in contrast to the viscosity of high concentration hemoglobin solutions: Hemoglobin molecules were designed by evolution to operate in environments where their concentration is very high, 35% (w/v) in the red cell cytosol, yet remain nonaggregated and preserve the flexibility of the red cell as it squeezes and slithers along the narrow capillaries. Hence, the hemoglobin molecules exhibit weak repulsion,[85,86] and the mutation in sickle cell hemoglobin that enables the formation of the polymers only induces a very short-range attraction.[86] The long-range repulsion underlies the unusually low viscosity of native and mutant hemoglobins even at the high concentration in the red cell cytosol,[87,88] or in the dense liquid phase. On the other hand, attraction is the dominant force acting between pairs of molecules in crystallizing protein solutions, and correspondingly, we expect high viscosity in the respective dense phases. Such high viscosity would arrest nucleation.

10. Nucleation of Ordered Solids as Superposition of Fluctuations along Two Order Parameters

As discussed above, the formation of crystals from solution should be viewed as a transition along two order parameters: density and "structure".[20] A "pure" density fluctuation may or may not lead to the formation of a long-lifetime, detectable droplet of dense liquid depending on the region of the phase diagram in which it occurs. Above the L−L coexistence line, all density fluctuations decay. In the region between the L−L binodal and L−L spinodal, only density fluctuations exceeding the critical size and amplitude, see Figure 2, lead to nuclei of dense liquid droplets. Below the L−L spinodal, all density fluctuations, even those of infinitesimal amplitude result in formation of a new liquid phase.

"Pure" structure fluctuations are only possible in melts, whose density is similar to that of the emerging crystalline phase. In a solution supersaturated with respect to the crystalline phase, a structure fluctuation

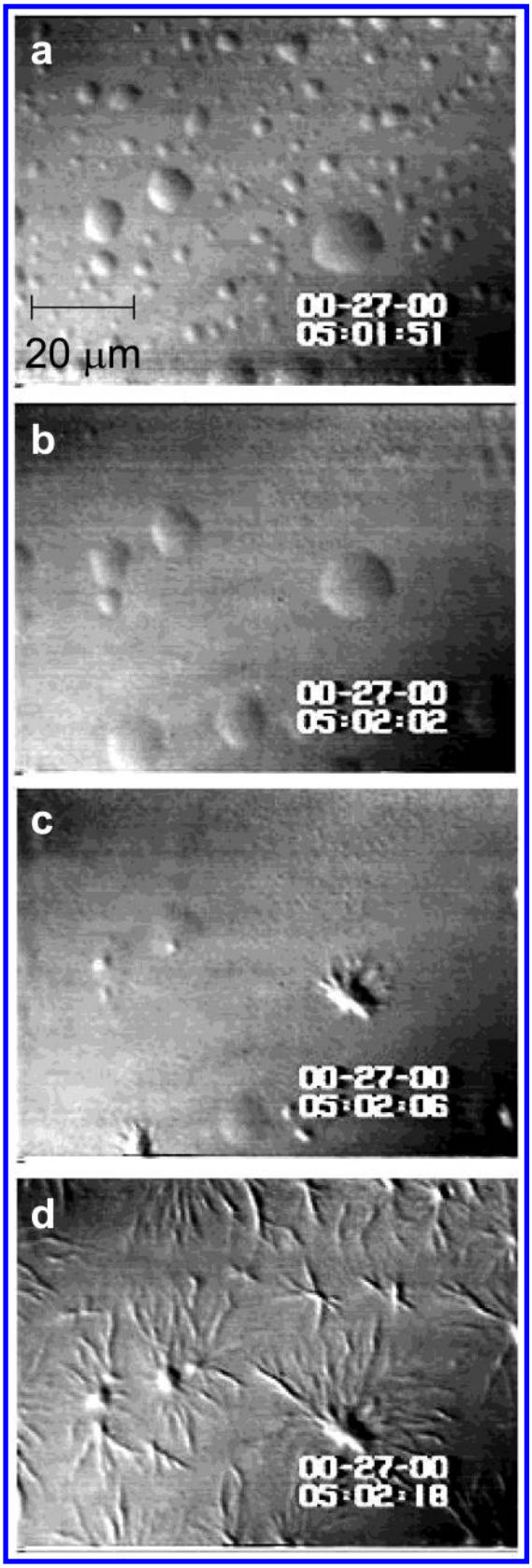

Figure 14. Link between L−L separation and formation of ordered linear arrays in deoxy-HbS solutions. Concentration of HbS is 22 g dL^{-1}. (a−d) When temperature is lowered from 42 to 35°C, the smaller of the dense liquid droplets disappear, while the larger ones serve as nucleation centers for HbS spherulites. Spherulites also appear at the locations where smaller droplets have been, apparently because of the undissipated locally higher concentration. Reprinted with permission from ref 84. Copyright 2002.

may lead to the formation of an ordered crystalline nucleus. The smallest fluctuation can be viewed as a pair of atoms or molecules from the melt that has an orientation similar to the orientation of a pair of atoms or molecules in the crystal; for informative examples, see refs 89 and 90. This crystals-like orientation in the pair is preserved over times significantly longer than the lifetime of a "bond" in the melt. The amplitude increase of a structure fluctuation occurs via the accumulation of such ordered pairs into an ordered piece of new phase. In a sense, structure fluctuations can be viewed as fluctuations of the density of ordered pairs. A key distinction between density and structure fluctuations is that structure fluctuations occur in a multidimensional space. They probe many different structures and if these structures have higher free energy than the melt the fluctuations inevitable decay. Only fluctuations that lead to a structure, which lowers the total free energy of the system may, after overcoming a barrier, become nuclei of an ordered phase with the selected structure.

For ordered solid phases nucleating not from their melt, but from a dilute solution or gas, a density and a structure fluctuation are needed so that a crystalline nucleus may form.

The results discussed above allow us to put forth a two-step mechanism of nucleation of crystals from solution illustrated in Figure 15. The main features of this mechanism are a density and a structure fluctuation that result in a crystalline nucleus occuring not simultaneously, but in sequence. The structure fluctuation is superimposed on the density fluctuation in such a way that during the lifetime of a density fluctuation, as it grown and decays, the material in the quasi-droplet may attain structure. Furthermore, there exists a density fluctuation with optimal size and density, which provide the highest probability that a structure fluctuation may occur in the quasi-droplet. Density fluctuations of larger sizes and amplitudes may spend less time in the optimal parameter region and decrease the probability of superposition of a structure fluctuation. Thus, to overcome their barrier and become crystalline nuclei, structure fluctuations do not require (i) long-lifetime droplets, such as those exiting below the L−L separation line or (ii) density fluctuations of large amplitude, such as those in the critical region. On the other hand, (iii) density fluctuations occurring below the L−L coexistence line lead to droplets that may never become crystals.

This mechanism well fits the experimental data. Indeed, the relative distance of the operating point of the system from the L−L coexistence line in the plane of the phase diagram in Figure 9 determines the prevailing sizes and the amplitudes of the density fluctuations. This is why the behavior of the $J(T)$ curves is correlated with the $T_{L-L}(C)$. Furthermore, the existence of optimal size and amplitude of the density fluctuation explains why the strongest enhancement of the nucleation of crystals does not occur at the spinodal for L−L separation, where the density fluctuations are strongest. Since the optimal density fluctuation may occur above the L−L coexistence line, we understand why the strongest enhancement and the $J(T)$ maximum are located above this line.

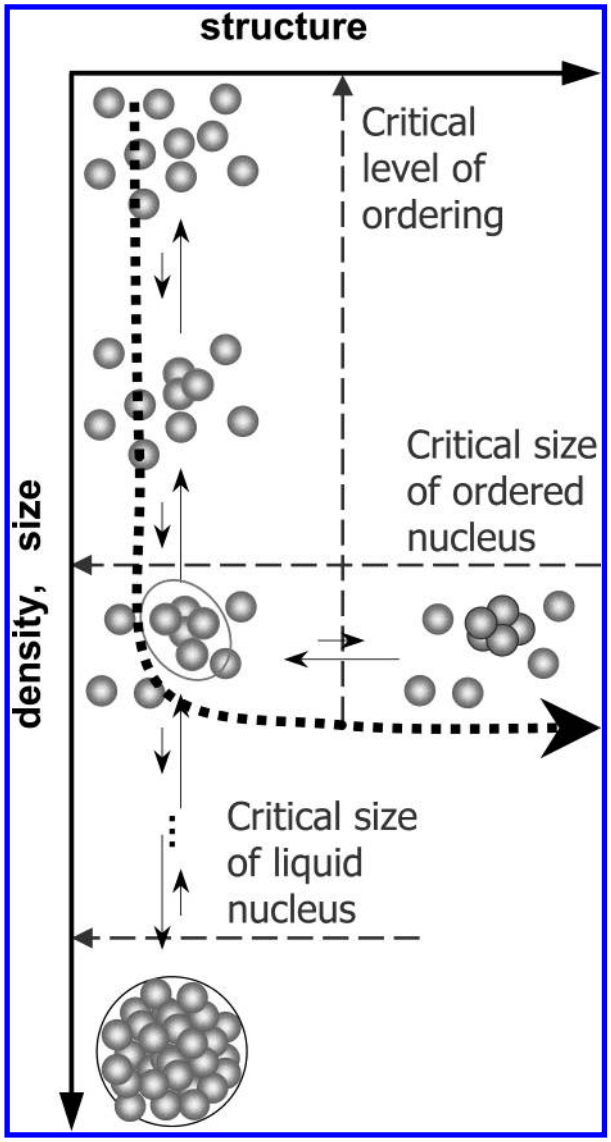

Figure 15. A schematic illustrating the formation of ordered crystalline nuclei as a result of the superposition of a density and a structure fluctuations. This schematic corresponds to a location in the phase diagram just below the L−L coexistence lines. At locations between the liquidus and the L−L coexistence lines, the critical liquid nucleus size is infinite, i.e., no density fluctuation can lead to a long-lifetime droplet. At locations between below the L−L spinodal line, any density fluctuation leads to a such a long-lifetime droplet.

For the investigated lysozyme system, the optimal density fluctuation occurs above the L−L coexistence line. Note that density fluctuations occur in all solutions, even in those in which L−L separation cannot be observed either because of the instability of a potential dense liquid phase, or of a short lifetime of a metastable dense liquid. Thus, the nucleation mechanism via the superposition of density and structure fluctuations may operate even for systems, for which dense liquid phases have never been observed.[24]

11. Control of Nucleation

The capability to enhance or suppress the rate of nucleation of protein crystals opens broad avenues in the area of protein crystallization for X-ray structure studies.[91] For instance, in some cases, the high supersaturations needed to achieve crystal nucleation lead to fast growth of poor-quality crystals.[4] Seeding can in some cases help to circumvent the problem;[92−94] however, often the surface of the seeds is contaminated or otherwise pacified and the technique is inapplicable. If protein crystal nucleation could be enhanced, this would allow crystal nucleation to occur at lower supersaturations, at which growth of higher-quality crystals may be expected. In other cases, new crystals are continuously nucleated throughout a crystallization run and may be incorporated into previously nucleated, larger crystals. Such incorporation may remain undetected and lead to mosaicity and lattice strain. Hence, for systems of this latter type, suppression of the secondary nucleation events should contribute to higher perfection. Control of protein crystal nucleation is needed in other health-related areas: production of protein crystalline pharmaceuticals,[2] protein separation,[95] and treatment of protein condensation diseases.[5,65,96−98]

Control of the spatial distribution, of the orientation and polymorphism is sought if crystals of microcrystalline particles are to be used in devices.[24,99,100]

The realization that the nucleation of ordered solid phases occurs as a superposition of fluctuations along two order parameters offers two handles for control of the spatiotemporal characteristics of nucleation—its rate and the distribution and orientation of the nuclei. The first one involves enhancing the desired structure fluctuation in the quasi-droplet comprising the density fluctuation. This has been done by applying electric field to a supersaturated solution. In one instance, a flat microscope slide with supersaturated solution of the protein lysozyme was placed between two electrodes and a field of ∼1500 V cm^{-1} was imposed.[31] It was found that the nucleation rate increased significantly, and that the crystals were preferentially oriented with their *c*-axis along the field lines. While the crystal orientation could be due to rotation of the crystallites after nucleation, the increased rate of nucleation suggests that the electric field stabilizes some of the structures that form and decay within a density fluctuation quasi droplet, and the stabilized structures are compatible with those leading to a crystalline nucleus. Note that orienting the protein molecules in the direction of the field should lead to suppression of nucleation—in tetragonal crystals, the molecules are oriented along symmetrically distributed angles along all three axes.

In another series of experiments, high power laser pulses were shone on supersaturated solutions of glycine.[24] It was found that the nucleation rate increases as a result of the illumination by 8−9 orders of magnitude and that by using elliptically or linearly polarized light, α- or γ-glycine crystals could be preferentially nucleated. Since glycine does not absorb the illumination wavelength, and the electric field intensity was insufficient to orient single glycine molecules, it was concluded that the elliptically or linearly polarized pulses stabilize the structure fluctuations leading to the respective solid phases, and in this way help the selection of the polymorph and speed up the rate of nucleation.[24,101]

Another way to control nucleation, suggested by the superposition mechanism, is by shifting the L−L coex-

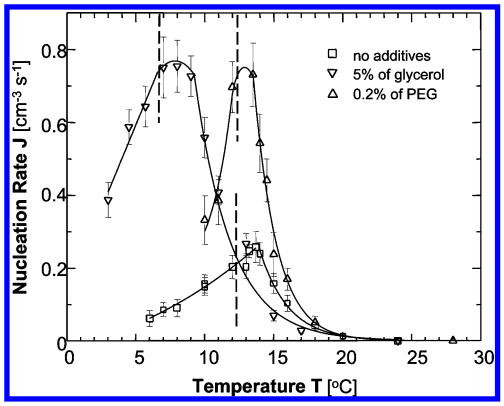

Figure 16. Dependencies of the rate of homogeneous nucleation of lysozyme crystals J on temperature T at pH = 4.5 by 50 mM sodium acetate buffer and 4% (w/v) NaCl. □ − lysozyme concentration C_{lys} = 50 mg/mL, no additives; ▽ − lysozyme concentration C_{lys} = 50 mg/mL, 5% (vol) glycerol, △ − C_{lys} = 50 mg/mL, 0.2% (w/v) poly(ethylene glycol) 5000. Vertical dotted lines indicate respective temperatures of L−L separation T_{L-L}. Curves are just guides for the eyes. Reprinted with permission from ref 72. Copyright 2000.

istence line and in this way controlling the density fluctuations.

12. Nucleation Control by Shifting T_{L-L}

The finding of a maximum in crystal nucleation rate near the L−L separation boundary suggests that shifting this boundary to lower temperatures can reduce J. One may attempt this by increasing the repulsion between the protein molecules.[62,74,102] Recent work with a trypsin inhibitor suggests that glycerol increases such repulsion.[103] Glycerol is preferentially rejected from the surroundings of the protein molecules,[104] stabilizes their native structures,[105] and enhances their folding in aqueous media.[106] The $J(T)$ curve in the presence of glycerol in Figure 16 shows that, indeed, T_{L-L} is lowered by 5 °C, see also Figure 17, and, at temperatures above the T_{L-L} for solutions sans glycerol, the nucleation rate is lowered by a factor of about three. Note that this suppression cannot be attributed to viscosity increases due to the glycerol: 5% glycerol causes a viscosity higher by only ∼13%,[107] which should affect the nucleation rate by the same factor.[17]

In other applications, enhancement of crystal nucleation is sought. Poly(ethylene glycol) (PEG) has been expected to increase the attraction between colloid particles solely due to the system's drive to minimize the excluded volume inaccessible to the polymer between two particles, often called depletion attraction.[62,102,108,109] It has been suggested that such nonadsorbing, nonbridging polymers should enhance nucleation.[19] The data on $J(T)$ in the presence of 0.2% (w/v) PEG with molecular mass 5000 Da (PEG 5000) are shown in Figure 16. This low concentration of PEG does not measurably affect the solubility or the L−L separation points, Figure 18.[72] Despite that, the rate of nucleation is increased 3-fold at T_{L-L} and less than that at higher or lower T's. Using PEG of various molecular masses in concentrations higher than 0.5% resulted in very fast nucleation often accompanied by solution gelation or amorphous precipitation of the protein, indicating strong isotropic intermolecular attraction.[26]

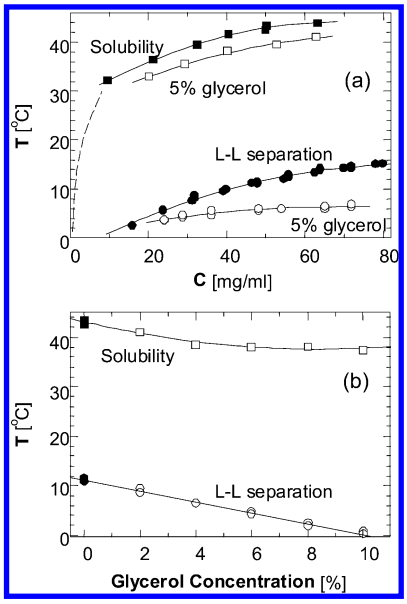

Figure 17. Effects of glycerol on the phase diagram of a lysozyme solution containing 4% (w/v) NaCl with a pH = 4.5 by 50 mM sodium acetate buffer. (a) Changes in the solubility and L−L separation boundaries introduced by the addition of 5% (vol) glycerol. Dashed line − solubility from ref 71. (b) Dependence of the solubility and L−L separation temperatures on the concentration of glycerol in a 50 mg/mL lysozyme solution. Reprinted with permission from ref 72. Copyright 2000.

The effect of PEG on J is considerably stronger than that of glycerol. The phase diagram of the protein solution in the presence of PEG in Figure 18 shows that PEG effects cannot be understood simply in terms of enhanced attraction due to restricted volume accessible to nonadsorbing noninteracting polymers. Recent models and experiments,[62,110,111] allowing for interactions between the polymer molecules, predict that, as the PEG concentration increases into the semidilute regime (where the polymer coils overlap), the attraction between the protein molecules should gradually taper off. The emerging complex picture of the interactions in a PEG−protein system agrees with recent direct force measurements.[112] They show strong, nonentropic attraction at high polymer−protein separations, corresponding to low PEG concentrations, and strong repulsion at short separations. The conclusions of these studies may at least partially explain the strong action of PEG on the nucleation kinetics.

13. Conclusions and Perspectives for Future Work

Above, I have reviewed recent experimental results indicating that the nucleation of lysozyme, and many other protein and small-molecule crystals follows a mechanism whereby a structure fluctuation occurs within a region of higher density of molecules existing for a limited time due to a density fluctuation, i.e., a structure fluctuation is superimposed on a density fluctuation. The novel points introduced by these results are

(i) The structure fluctuation follows and is superimposed upon the density fluctuation, in contrast to a simultaneous fluctuations along both density and struc-

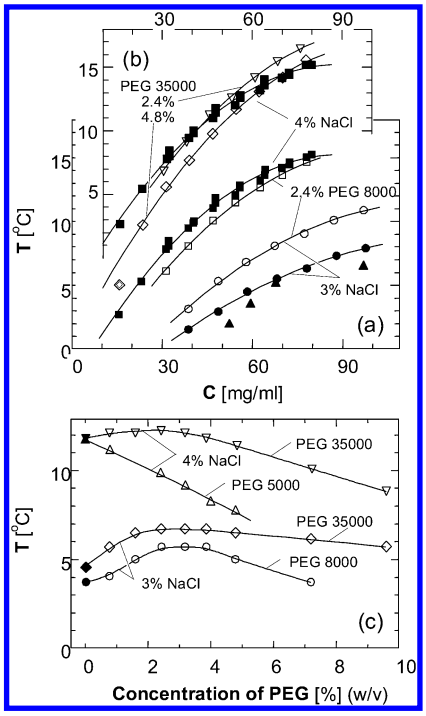

Figure 18. Effects of poly(ethylene glycol) (PEG) with molecular mass and concentration indicated in the plots on the L−L separation in a lysozyme solution containing 3 or 4% NaCl with a pH = 4.5 by 50 mM sodium acetate buffer. Full symbols − no additive; open symbols − PEG added as indicated in the plots. Curves are just guides for the eye. (a, b) Changes in the L−L separation boundary introduced by the addition of PEG. ▲ − data of ref 45 for 3% NaCl. (c) Dependence of the L−L separation temperature on the concentration of PEG in a 50 mg/mL lysozyme solution. Reprinted with permission from ref 72. Copyright 2000.

ture order parameters, implicitly assumed in earlier crystal nucleation theories.

(ii) The fluctuations along the two order parameters occur in sequence in broad areas of phase space and not only around the critical point for L−L separation, as suggested by a pioneering theory on the subject.

(iii) The density fluctuation may result in a long-lifetime dense liquid phase, metastable with respect to the crystals, but stable with respect to the low-density solution, or in a short lifetime state, metastable with respect to both the low-density solution and the crystals. For many systems, long-lifetime dense liquids actually arrest the nucleation of crystals, likely due to their high viscosity.

(iv) The realization of the role of the doubly metastable state, the dense liquid quasi-droplet, for the nucleation of crystals is one of the main conclusions of the results reviewed here. It shows that nucleation of crystals occurs as a sequential superposition of fluctuations not only in the vicinity of the L−L coexistence area, but also away from it, and even for system in which L−L separation is not observed.

The outlook on crystal nucleation as a superposition of a density and a structure fluctuation suggests two major pathways of nucleation control. The first one is based on affecting the frequency and amplitudes of density fluctuations through the intermolecular interactions in solution. Thus, increasing the attraction between solute molecules enhances the density fluctuations and increases the nucleation rate, while stronger repulsion leads to weaker density fluctuations and lower nucleation rates. The second control pathway involves increasing the probability of a structure fluctuation toward a crystal structure that lowers the total free energy. For this, anisotropic optical and electric fields have been used. Other possibilities include the use of suitable templates, etc.

Many questions related to the proposed mechanism are still to be addressed. Among them are

(i) What are the relative heights of the free energy barriers that the density and the structure fluctuations overcome in the nucleation reaction pathway?

(ii) The most general nucleation rate low is written as a product of a Boltzmann-type exponential factor containing the free energy barrier for nucleation and a preexponential factor accounting for the kinetics of assembly of the critical cluster. Obviously, such a simple expression will not be valid for nucleation that follows a two-step mechanism. One would expect a combination of preexponential and Boltzmann-type factors for each of the steps in the nucleation mechanism. What would the concrete form of this expression be?

(iii) What is the role of the kinetic factors, typically accounted for by the preexponential factors in the nucleation rates expressions, for the rate of growth of the density and the structure fluctuations?

The fast nucleation of liquid droplets suggest that the combination of preexponential kinetic factors and free energy barrier for the density fluctuations is such they are significantly faster than the structure fluctuations. However, the relative importance of the barrier and the preexponential factors for the growth rate of the structure fluctuations is an open question of high consequence.

Other issues include:

(i) The nucleation theorem, linking the nucleation barrier to the nucleation driving force via the size of the critical nucleus has only been derived for systems for which nucleation occurs in a single step. The validity and form of the nucleation theorem for the two-step mechanism discussed here have not been examined.

(ii) A concise theory accounting for the main parameters that determine the probability and amplitudes of the sequential density and structure fluctuation needs to be developed.

(iii) Experimental and theoretical work that would elucidate the role of the viscosity of the dense liquid intermediate is needed.

(iv) A rationalization of the nucleation via critical clusters consisting of one molecule, occurring at high supersaturation is needed. The barriers for such nucleation are lower than the thermal energy of the molecules and, correspondingly, its rate is only limited by the kinetics of assembly of the molecules. This is very similar to spinodal decomposition;[12,113] however, the theoretical concepts needed for the understanding of a spinodal decomposition during a phase transition along two order parameter are barely nascent.[114,115]

Acknowledgment. My deepest gratitude goes to my collaborators, without whom the investigations that comprise the bulk of the material reviewed here and

serve as the basis for the formulation of the main ideas in this review would have been impossible, O Galkin and D. N. Petsev. I have benefited from numerous insightful discussions with A. Kolomeisky, G. Nicolis, D. Frenkel, and D. Oxtoby on the subject. Generous financial support over the years was provided by the National Lung, Heart and Blood Institute, NIH, and the Office of Biological and Physical Research, NASA.

References

(1) Lasaga, A. C.; Lüttge, A. *Science* **2001**, *291*, 2400.
(2) Brange, J. *Galenics of Insulin*; Springer: Berlin, 1987.
(3) Shi, B.; Rousseau, R. W. *Ind. Eng. Chem. Res.* **2001**, *40*, 1541.
(4) McPherson, A. *Crystallization of Biological Macromolecules*; Cold Spring Harbor Laboratory Press: Cold Spring Harbor New York, 1999.
(5) Eaton, W. A.; Hofrichter, J. Sickle cell hemoglobin polimerization. In *Advances in Protein Chemistry*; Anfinsen, C. B., Edsal, J. T., Richards, F. M., Eisenberg, D. S., Eds.; Academic Press: San Diego, 1990; Vol. 40, p 63.
(6) Asherie, N.; Pande, J.; Pande, A.; Zarutskie, J. A.; Lomakin, J.; Lomakin, A.; Ogun, O.; Stern, L. J.; King, J.; Benedek, G. B. *J. Mol. Biol.* **2001**, *314*, 663.
(7) Gibbs, J. W. *Trans. Connect. Acad. Sci.* **1876**, *3*, 108.
(8) Gibbs, J. W. *Trans. Connect. Acad. Sci.* **1878**, *16*, 343.
(9) Hohenberg, P. C.; Halperin, B. I. *Rev. Mod. Phys.* **1977**, *49*, 435.
(10) Chaikin, P. M.; Lubensky, T. C. *Principles of Condensed Matter Physics*; Cambridge Unversity Press: Cambridge, 1995.
(11) Kashchiev, D. *Nucleation. Basic Theory with Applications*; Butterworth: Heinemann: Oxford, 1999.
(12) Binder, K.; Fratzl, P. Spinodal decomposition. In *Phase Transformation in Materials*; Kostorz, G., Ed.; Wiley: New York, 2001.
(13) Kashchiev, D. *J. Chem. Phys.* **2003**, *118*, 1837.
(14) Katz, J. L.; Ostermier, B. J. *J. Chem. Phys.* **1967**, *47*, 478.
(15) Neilsen, A. E. Nucleation in aqueous solutions. In *Crystal Growth*; Peiser, S., Ed.; Pergamon: Oxford, 1967; p 419.
(16) Kahlweit, M. Nucleation in Liquid solutions. In *Physical Chemistry*; Eyring, H., Ed.; Academic Press: New York, 1969; Vol. VII, p 675.
(17) Walton, A. G. Nucleation in liquids and solutions. In *Nucleation*; Zettlemoyer, A. C., Ed.; Marcel Dekker: New York, 1969; p 225.
(18) Landau, L. D.; Lifschitz, L. *Statistical Physics, Part 1*, 3rd ed.; Pergamon Press: Oxford, 1977; Vol. 5.
(19) ten Wolde, P. R.; Frenkel, D. *Science* **1997**, *277*, 1975.
(20) Talanquer, V.; Oxtoby, D. W. *J. Chem. Phys.* **1998**, *109*, 223.
(21) Soga, K. G.; Melrose, J. M.; Ball, R. C. *J. Chem. Phys.* **1999**, *110*, 2280.
(22) Thomson, J. A.; Schurtenberger, P.; Thurston, G. M.; Benedek, G. B. *Proc. Natl. Acad. Sci. U.S.A.* **1987**, *84*, 7079.
(23) Asherie, N.; Lomakin, A.; Benedek, G. B. *Phys. Rev. Lett.* **1996**, *77*, 4832.
(24) Garetz, B.; Matic, J.; Myerson, A. *Phys. Rev. Lett.* **2002**, *89*, 175501.
(25) Bonnett, P. E.; Carpenter, K. J.; Dawson, S.; Davey, R. J. *Chem. Commun.* **2003**, 698.
(26) Sear, R. P. *J. Chem. Phys.* **1999**, *111*, 4800.
(27) Hung, C.-H.; Krasnopoler, M. J.; Katz, J. L. *J. Chem. Phys.* **1989**, *90*, 1856.
(28) Bartell, L. S.; Dibble, T. S. *J. Phys. Chem.* **1991**, *95*, 1159.
(29) Arnold, S.; Goddard, N. L.; Wotherspoon, N. *Rev. Sci. Instrum.* **1999**, *70*, 1473.
(30) Izmailov, A. F.; Myerson, A. S.; Arnold, S. *J. Cryst. Growth* **1999**, *196*, 234.
(31) Nanev, C. N.; Penkova, A. *J. Cryst. Growth* **2001**, *232*, 285.
(32) Kam, Z.; Shore, H. B.; Feher, G. *J. Mol. Biol.* **1978**, *123*, 539.
(33) Vekilov, P. G.; Monaco, L. A.; Thomas, B. R.; Stojanoff, V.; Rosenberger, F. *Acta Crystallogr. Sect. D* **1996**, *52*, 785.
(34) Judge, R. A.; Jacobs, R. S.; Frazer, T.; Snell, E. H.; Pusey, M. L. *Biophys. J.* **1999**, *77*, 1585.
(35) Burke, M. W.; Judge, R. A.; Pusey, M. L. *J. Cryst. Growth* **2001**, *232*, 301.
(36) Sazaki, G.; Yoshida, E.; Komatsu, H.; Nakada, T.; Miyashita, S.; Watanabe, K. *J. Cryst. Growth* **1997**, *173*, 231.
(37) Vekilov, P. G.; Galkin, O. *Colloids Surf., A* **2003**, *215*, 125.
(38) Malkin, A. J.; McPherson, A. *J. Cryst. Growth* **1993**, *128*, 1232.
(39) Malkin, A. J.; McPherson, A. *Acta Crystallogr. Sect. D* **1994**, *50*, 385.
(40) Tammann, G. *Die Aggregatzustaende*, 2nd ed.; Voss: Leipsig, 1922.
(41) Chayen, N. E. *J. Cryst. Growth* **1999**, *196*, 434.
(42) Galkin, O.; Vekilov, P. G. *J. Phys. Chem.* **1999**, *103*, 10965.
(43) Galkin, O.; Vekilov, P. G. *J. Am. Chem. Soc.* **2000**, *122*, 156.
(44) Muschol, M.; Rosenberger, F. *J. Chem. Phys.* **1995**, *103*, 10424.
(45) Muschol, M.; Rosenberger, F. *J. Chem. Phys.* **1997**, *107*, 1953.
(46) Gibbs, J. W. *The Collected Works of J. W. Gibbs*; Yale University Press: New Haven, 1961; Vol. 1.
(47) Volmer, M. *Kinetik der Phasenbildung*; Steinkopff: Dresden, 1939.
(48) Oxtoby, D. W. *J. Phys.: Condens. Matter* **1992**, *4*, 7627.
(49) Oxtoby, D. W. *Acc. Chem. Res.* **1998**, *31*, 91.
(50) Kashchiev, D. *J. Chem. Phys.* **1982**, *76*, 5098.
(51) Oxtoby, D. W.; Kashchiev, D. *J. Chem. Phys.* **1994**, *100*, 7665.
(52) Milchev, A. *Contemp. Phys.* **1991**, *32*, 321.
(53) Milchev, A. *Elecrocrystallization: Fundamentals of Nucleation and Growth*; Kluwer: Dordrecht, The Netherlands, 2002.
(54) Mutaftschiev, B. Nucleation theory. In *Handbook of Crystal Growth*; Hurle, D. T. J., Ed.; Elsevier: Amsterdam, 1993; Vol. I; p 189.
(55) Turnbull, D.; Fisher, J. C. *J. Chem. Phys.* **1949**, *17*, 71.
(56) Laaksonen, A.; Telaquer, V.; Oxtoby, D. W. *Annu. Rev. Phys. Chem.* **1995**, *46*, 489.
(57) Schenter, G. K.; Kathmann, S. M.; Garrett, B. C. *Phys. Rev. Lett.* **1999**, *82*, 3483.
(58) McGraw, R.; Laaksonen, A. *Phys. Rev. Lett.* **1996**, *76*, 2754.
(59) Casselyn, M.; Perez, J.; Tardieu, A.; Vachette, P.; Witz, J.; Delacroix, H. *Acta Crystallogr., Sect. D: Biol. Crystallogr.* **2001**, *57*, 1799.
(60) Tardieu, A.; Verge, A. L.; Malfois, M.; Bonnette, F.; Finet, S.; Ries-Kaut, M.; Belloni, L. *J. Cryst. Growth* **1999**, *196*, 193.
(61) Rosenbaum, D. F.; Zamora, P. C.; Zukoski, C. F. *Phys. Rev. Lett.* **1996**, *76*, 150.
(62) Gast, A. P.; Hall, C. K.; Russel, W. R. *Faraday Discuss. Chem. Soc.* **1983**, *76*, 189.
(63) Hagen, M. H. J.; Frenkel, D. *J. Chem. Phys.* **1994**, *101*, 4093.
(64) Poon, W. C. K.; Pirie, A. D.; Pusey, P. N. *Faraday Discuss.* **1995**, *101*, 65.
(65) Broide, M. L.; Berland, C. R.; Pande, J.; Ogun, O. O.; Benedek, G. B. *Proc. Natl. Acad. Sci. U.S.A.* **1991**, *88*, 5660.
(66) Berland, C. R.; Thurston, G. M.; Kondo, M.; Broide, M. L.; Pande, J.; Ogun, O.; Benedek, G. B. *Proc. Natl. Acad. Sci. U.S.A.* **1992**, *89*, 1214.
(67) Broide, M. L.; Tominc, T. M.; Saxowsky, M. D. *Phys. Rev. E* **1996**, *53*, 6325.
(68) Hagen, M.; Meijer, E.; Mooij, G.; Frenkel, D.; Lekkerkerker, H. *Nature* **1993**, *365*, 425.
(69) Noro, M. G.; Kern, N.; Frenkel, D. *Europhys. Lett.* **1999**, *48*, 332.
(70) Atkins, P. *Physical Chemistry*, 6th ed.; Freeman: New York, 1998.
(71) Cacioppo, E.; Pusey, M. L. *J. Cryst. Growth* **1991**, *114*, 286.
(72) Galkin, O.; Vekilov, P. G. *Proc. Natl. Acad. Sci. U.S.A.* **2000**, *97*, 6277.
(73) SanBiagio, P. L.; Palma, M. U. *Biophys. J.* **1991**, *60*, 508.
(74) Evans, R. M. L.; Poon, W. C. K.; Gates, M. E. *Europhys. Lett.* **1997**, *38*, 595.
(75) Anderson, V. J.; Lekkerkerker, H. N. W. *Nature* **2002**, *416*, 811.
(76) Haas, C.; Drenth, J. *J. Phys. Chem.* **2000**, *104*, 358.
(77) Lomakin, A.; Asherie, N.; Benedek, G. B. *J. Chem. Phys.* **1996**, *104*, 1646.
(78) Lomakin, A.; Asherie, N.; Benedek, G. *Proc. Natl. Acad. Sci. U.S.A.* **1999**, *96*, 9465.

(79) Kuznetsov, Y. G.; Malkin, A. J.; McPherson, A. *J. Cryst. Growth* **2001**, *232*, 30.
(80) *Disorders of Hemoglobin: Genetics, Pathology, Clinical Management*; Steinberg, M. H.; Forget, B. G.; Higgs, D. R.; Nagel, R. L., Eds.; Cambridge University Press: Cambridge, 2000.
(81) Cole-Strauss, A.; Yoon, K.; Xiang, Y.; Byrne, B. C.; Rice, M. C.; Crynn, J.; Holloman, W. K.; Kmiec, E. B. *Science* **1996**, *273*, 1386.
(82) Hahn, E. V.; Gillespie, E. B. *Arch. Int. Med.* **1927**, *39*, 233.
(83) Sunshine, H. R.; Hofrichter, J.; Ferrone, F. A.; Eaton, W. A. *J. Mol. Biol.* **1982**, *158*.
(84) Galkin, O.; Chen, K.; Nagel, R. L.; Hirsch, R. E.; Vekilov, P. G. *Proc. Natl. Acad. Sci. U.S.A.* **2002**, *99*, 8479.
(85) Minton, A. P. *J. Mol. Biol.* **1977**, *110*, 89.
(86) Vekilov, P. G.; Feeling-Taylor, A. R.; Petsev, D. N.; Galkin, O.; Nagel, R. L.; Hirsch, R. E. *Biophys. J.* **2002**, *83*, 1147.
(87) Briehl, R. W. *Am. J. Pediatr. Hematol. Oncol.* **1983**, *5*, 390.
(88) Briehl, R. W.; Nikopoulou, P. *Blood* **1993**, *81*, 2420.
(89) Gasser, U.; Weeks, E.; Schofield, A.; Pusey, P.; Weitz, D. *Science* **2001**, *292*, 258.
(90) Matsumoto, M.; Saito, S.; Ohmine, I. *Nature* **2002**, *416*, 409.
(91) Weber, P. C. Overview of protein crystallization methods. In *Methods in Enzymology*; Carter, Jr., C. W., Sweet, R. M., Eds.; Academic Press: New York, 1997; Vol. 276, p 13.
(92) Stura, E. A.; Wilson, I. A. Seeding techniques. In *Crystallization of Nucleic Acids and Proteins: A Practical Approach*; Ducruix, A., Giege, R., Eds.; Oxford University Press: Oxford, 1992; p 99.
(93) Stura, E. A.; Satterwait, A. C.; Calvo, J. C.; Carslow, D. C.; Wilson, I. A. *Acta Crystallogr. Sect. D* **1994**, *50*, 448.
(94) Stura, E. A.; Charbonnier, J.-B.; Taussig, M. J. *J. Cryst. Growth* **1999**, *196*, 250.
(95) Mahadevan, H.; Hall, C. K. *AIChE J.* **1992**, *38*, 573.
(96) Lomakin, A.; Chung, D. S.; Benedek, G. B.; Kirschner, D. A.; Teplow, D. B. *Proc. Natl. Acad. Sci. U.S.A.* **1996**, *93*, 1125.
(97) Kusimoto, Y.; Lomakin, A.; Teplow, D. P.; Benedek, G. B. *Proc. Natl. Acad. Sci. U.S.A.* **1998**, *95*, 12277.
(98) Zastavker, Y. V.; Asherie, N.; Lomakin, A.; Pande, J.; Donovan, J. M.; Schnur, J. M.; Benedek, G. B. *Proc. Natl. Acad. Sci. U.S.A.* **1999**, *96*, 7883.
(99) Aizenberg, J.; Black, A. J.; Whitesides, G. M. *Nature* **1999**, 495.
(100) Weissbuch, I.; Lahav, M.; Leiserowitz, L. *Cryst. Growth Des.* **2003**, *3*, 125.
(101) Oxtoby, D. W. *Nature* **2002**, *420*, 277.
(102) Illett, S. M.; Orrock, A.; Poon, W. C. K.; Pusey, P. N. *Phys. Rev. E* **1995**, *51*, 1344.
(103) Farnum, M.; Zukoski, C. *Biophys. J.* **1999**, *76*, 2716.
(104) Gekko, K.; Timasheff, S. N. *Biochemistry* **1981**, *20*, 4667.
(105) Sousa, R. *Acta Crystallogr., Sect. D* **1995**, *51*, 271.
(106) Rariy, R. V.; Klibanov, A. M. *Proc. Natl. Acad. Sci. U.S.A.* **1997**, *94*, 13520.
(107) *Landoldt-Bornstein Numerical Data and Functional Relationships. Vol. IV, Part II. Materials Values and Mechanical Behaviour of Nonmetals*; Borchers, H., Ed.; Springer: Berlin, 1955.
(108) Asakura, S.; Oosawa, F. *J. Polym. Sci.* **1958**, *33*, 183.
(109) Verma, R.; Crocker, J. C.; Lubensky, T. C.; Yodh, A. G. *Phys. Rev. Lett.* **1998**, *81*, 4004.
(110) Chatterjee, A. P.; Schweizer, K. S. *J. Chem. Phys.* **1998**, *109*, 10464.
(111) Kulkarni, A. M.; Chatterjee, A. P.; Schweitzer, K. S.; Zukoski, C. F. *Phys. Rev. Lett.* **1999**, *83*, 4554.
(112) Sheth, S. R.; Leckband, D. *Proc. Natl. Acad. Sci. U.S.A.* **1997**, *94*, 8399.
(113) Cahn, J. W.; Hilliard, J. E. *J. Chem. Phys.* **1958**, *28*, 258.
(114) Flory, P. J. *Statistical Mechanics of Chain Molecules*; Wiley: New York, 1969.
(115) Dorgan, J. R.; Yan, D. *Macromolecules* **1998**, *31*, 193.
(116) Petsev, D. N.; Wu, X.; Galkin, O.; Vekilov, P. G. *J. Phys. Chem. B* **2003**, *107*, 3921.
(117) Feeling-Taylor, A. R.; Banish, R. M.; Hirsch, R. E.; Vekilov, P. G. *Rev. Sci. Instrum.* **1999**, *70*, 2845.

CG049977W